Understanding the Mechanochemistry of Ladder-Type Cyclobutane Mechanophores by Single Molecule Force Spectroscopy

Matías Horst, Jinghui Yang, Jan Meisner, Tatiana B. Kouznetsova, Todd J. Martínez,* Stephen L. Craig,* and Yan Xia*

ABSTRACT: We have recently reported a series of ladder-type cyclobutane mechanophores, polymers of which can transform from nonconjugated structures to conjugated structures and change many properties at once. These multicyclic mechanophores, namely, *exo*-ladderane/ene, *endo*-benzoladderene, and *exo*-bicyclohexene-*peri*-naphthalene, have different ring structures fused to the first cyclobutane, significantly different free energy changes for ring-opening, and different stereochemistry. To better understand their mechanochemistry, we used single molecule force spectroscopy (SMFS) to characterize their force−extension behavior and measure the threshold forces. The threshold forces correlate with the activation energy of the first bond, but not with the strain of the fused rings distal to the polymer main chain, suggesting that the activation of these ladder-type mechanophores occurs with similar early transition states, which is supported by force-modified potential energy surface calculations. We further determined the stereochemistry of the mechanically generated dienes and observed significant and variable contour length elongation for these mechanophores both experimentally and computationally. The fundamental understanding of ladder-type mechanophores will facilitate future design of multicyclic mechanophores with amplified force-response and their applications as mechanically responsive materials.

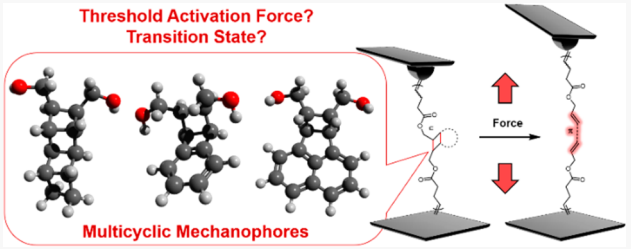

INTRODUCTION

Stress-induced nondestructive chemical transformations of mechanophores in polymers are of considerable interest to develop force-responsive materials and explore selective force-activated chemical pathways different from those of force-free thermally induced reactions. A fundamental understanding of mechanochemistry has significantly advanced on several fronts, exploring force-modified reaction pathways and reaction selectivity,[1−6] lever arm effects,[7,8] and dynamic effects.[9,10] The threshold force for activation of covalent bonds on a given time scale of interest is one of the most important parameters in mechanochemistry. To advance the design and development of mechanophores, it is important to understand how different molecular features affect the threshold force of mechanoactivation experimentally and computationally. However, the accurate prediction of such threshold force remains a challenge. Constrained geometries simulate external force (COGEF) models offer maximum force predictions that correlate with experimental threshold forces and have proven useful for predicting relative trends,[11,12] but they lack precise predictive power. Theoretical approaches to treat the influence of external forces on reactivity have advanced over the last two decades with increasing use of models that explicitly consider external forces and treat reactions under more realistic conditions.[13−16]

Four-membered rings are a common motif in the design of mechanophores. For example, Moore and co-workers showed that benzocyclobutenes (BCBs) can undergo force-induced ring opening contrary to the Woodward−Hoffmann thermal reactivity, and Craig and co-workers quantified the forces for ring opening of different substituted BCBs to be about 1−1.5 nN, dependent on the stereochemistry and structure of the substituents.[3,17] The Moore group also demonstrated that the ease of mechanoactivation depends on the number and stereochemistry of subsitutents.[18] Boulatov, Craig, and Weng have used mechanically active cyclobutane rings to gate the activity of a second mechanophore.[19,20]

Recently, we have reported several ladder-type mechanophores that contain multiple fused four-membered rings. Their polymers can be force-activated to transform from nonconjugated structures to conjugated structures and induce dramatic changes in many materials properties.[21−24] We developed three families of ladder-type cyclobutene mechano-

Received: June 6, 2021
Published: July 26, 2021

https://doi.org/10.1021/jacs.1c05857

phore monomers, [5]ladderene/ane,[10,21,22] benzoladderenes,[23] and bicyclohexene-*peri*-naphthalenes[24] with increasing synthetic scalability, functional group diversity, and thermal stability (Scheme 1). These monomers can be directly polymerized via ring-opening metathesis polymerization (ROMP) to produce polymechanophores in quantitative conversions. Upon sonication, ~40% repeat units of these polymechanophores can be activated to transform into conjugated structures.[21,23,24]

Scheme 1. Previously Reported Ladder-Type Cyclobutene Mechanophore Monomers and Their Polymers before and after Mechanoactivation[a]

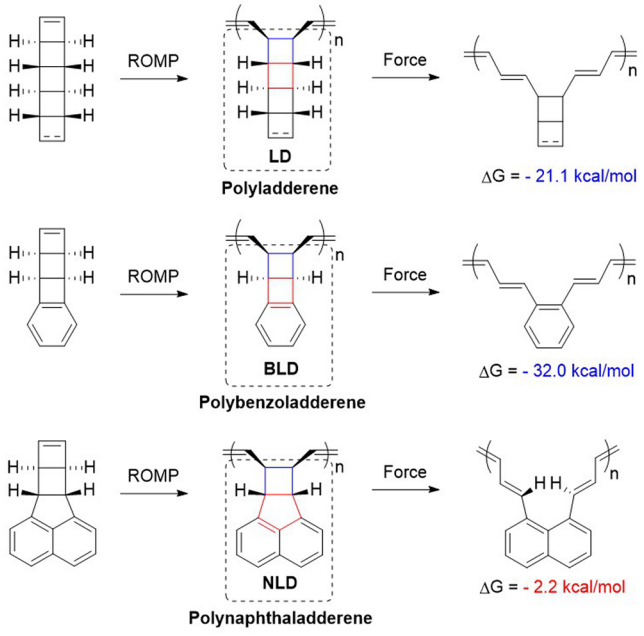

[a]The mechanophore repeat units are circled by dashed lines, and the calculated free energy changes (based on B3LYP-D3/6-31G(d) theory) upon ring opening of the first cyclobutane ring in these mechanophores under force-free conditions are shown.

A comparison of this series of ladder-type cyclobutane mechanophores will further our understanding of the mechanochemistry of such scaffolds. As described in Scheme 1, we categorize the mechanophore structures in the repeat units of these polymers as ladderane (**LD**), benzo-ladderane (**BLD**), and naphtha-ladderane (**NLD**), for convenience. The mechanoactivation of each mechanophore involves the ring-opening of the first cyclobutane ring in the polymer backbone, but several differences exist: (1) the second fused rings for **LD**, **BLD**, and **NLD** are a cyclobutane, a formal cyclobutene, and a five-membered ring, respectively. (2) The first cyclobutane ring in both **LD** and **NLD** has an *exo* configuration, while that in **BLD** has an *endo* configuration, as a result of their different syntheses. (3) The force-free free energy change of ring-opening, calculated via density functional theory (DFT) at the B3LYP-D3/6-31G(d) level, varies significantly and is −32.0, −21.1, and −2.2 kcal/mol for **BLD**, **LD**, and **NLD** with alkene substituents, respectively (Scheme 1 and Table S1). The almost thermodynamically neutral ring-opening of **NLD**, despite the release of ring strain, is presumably due to the steric clash of the generated diene at the *peri* positions of naphthalene. Under force-free conditions, one might therefore expect that the transition state would shift earlier on the reaction coordinate as the enthalpy of reaction becomes increasingly negative (or less positive), as predicted by the Hammond postulate. These differences in the structural features and energies of these three ladder-type mechanophores intrigued us to understand their effects on the threshold forces and mechanochemical reaction pathways.

RESULTS AND DISCUSSION

Ultrasonication, a commonly used technique for mechanoactivation, generates high strain rates and broad force distributions.[25,26] Here, we used single molecule force spectroscopy (SMFS) to directly measure the activation force in a kinetics regime relevant to mechanoactivation for most potential applications and provide information for comparison of reaction pathways across different mechanophores. SMFS has been used to study force-rate behavior and structure−reactivity relationships of mechanophores such as spiropyrans,[27,28] gem-dihalocyclopropanes,[8] benzocyclobutanes,[3] and organometallic complexes.[29−31]

We first needed to prepare mechanophore polymers suitable for SMFS. The Craig lab has incorporated epoxides in the polymer backbone to provide strong attachment to the atomic force microscope (AFM) tip to allow application of nN-regime forces that are high enough to mechanically activate covalent bonds. Since we have previously achieved controlled ROMP of the mechanophore monomers,[22−24] we partly epoxidized the backbone olefins of their resulting ROMP polymers or prepared triblock copolymers containing the mechanophore monomers flanked by short end blocks of norbornene containing an appendant epoxide group. However, in the many attempted SMFS experiments, these polymer designs gave very low rates of successful pulls that reached the plateau in the force curve that represents activation of multiple mechanophores. Even in the few occasions that a plateau was observed, the polymer chain broke from the tip or substrate surface before the plateau was completed, and not all mechanophores were activated prior to detachment (Figure S17). These observations are consistent with reported difficulties in SMFS characterization of other mechanophore systems with relatively high activation forces.[20,32] We also attempted copolymerization of the mechanophore monomers with cyclooctene epoxide via ROMP. The resulting copolymers still detached before full mechanophore activation was achieved (Figure S18).

Since Craig and co-workers have commonly used copolymers of macrocyclic mechanophores and cyclooctene epoxide for successful SMFS,[8,27] we adopted the same design to synthesize macrocycles containing each of the ladder mechanophores. We prepared the di(hydroxymethyl) derivative of each mechanophore, which was then functionalized with terminal alkenes (Scheme 2). The resulting dienes were cyclized to form 14-membered macrocycles in moderate yields under diluted conditions by ring closing metathesis. Finally, entropy-driven ROMP was used to prepare statistical copolymers of these macrocycles with epoxy-cyclooctene at varied ratios using the second generation Grubbs catalyst. All the mechanophore macrocycles gave similar M_n of 25−40 kDa and $Đ$ around 1.7 (Table 1). High polymer molar masses are desirable to ensure that each AFM pull could sample a large number of mechanophores along the same polymer chain and each chain has adequate substrate adhesion to reach the activation forces. The mechanophore comonomer composition

Scheme 2. Structure of ROMP Monomers and Synthesis of ED-ROMP Polymers for SMFS Characterization[a]

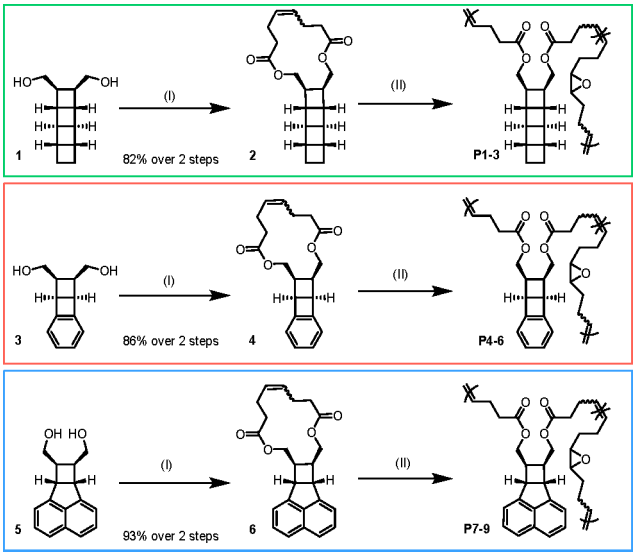

[a]Conditions: (I) Pentenoic anhydride (2.2 eq vs diol), EDC (1.5 equiv), DMAP (0.1 equiv), CH_2Cl_2, r.t.; then Hoveyda-Grubbs II (3 mol %), CH_2Cl_2 to 1 mM in substrate, r.t. (II) epoxy-cyclooctene, Grubbs II, $CHCl_3$, 40°C. Specified stereochemistry for **P1-9** refers only to that of the repeat unit, not the polymer tacticity. Comonomer ratio and M_n for **P1-9** are enumerated in Table 1.

was varied from 7% to 63% as determined by NMR spectroscopy to enable correlation of mechanophore content and the change in polymer contour length upon mechanoactivation. All the mechanophores have the same *syn* di-(methylcarboxylate) linkage to the polymer backbone, and the analogous design and synthesis of polymers ensured that the species being compared have the same polymer backbone structures and mechanophore linkage.

These polymers in dilute toluene solutions were adsorbed onto a silicon surface and then probed with a calibrated cantilever by nanofishing in a toluene flow cell at a cantilever retraction rate of 300 nm/sec. Delightfully, the flexible polymer backbone design proved effective at providing a strong binding of polymers to the AFM tip and substrate to capture the complete mechanochemical chain extension.

In the force–extension curve, each polymer exhibited a plateau characteristic of the change in contour length resulting from mechanophore activation (Figure 1), and the relative extension varied as a function of mechanophore and

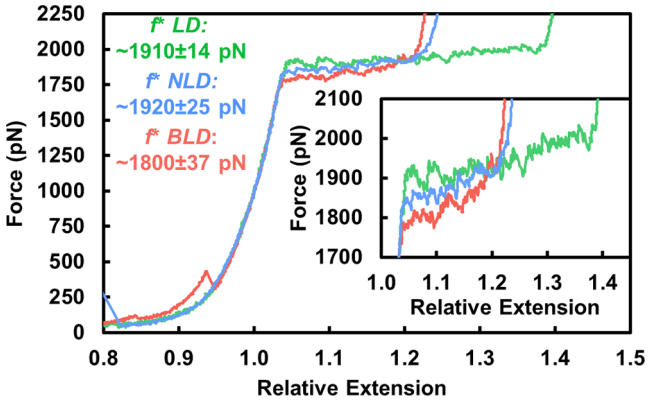

Figure 1. Representative force curves of **P3** (green), **P6** (red), and **P9** (blue) obtained by SMFS at a retraction velocity of 300 nm/s. Actual forces are obtained by averaging over many such curves, and actual changes in contour length are determined by fitting the pre- and post-transition regions of the force curves to extended freely jointed chain models.

mechanophore content. The force at the midpoint of the plateau region was taken as the threshold force.[33] The two mechanophores with an *exo* configuration, **LD** and **NLD**, exhibited similar threshold force of 1910 ± 14 and 1920 ± 25 pN, respectively. **BLD** exhibited a smaller threshold force of 1800 ± 37 pN. These values fall within the range of previously reported threshold forces for cyclobutane rings, such as 2.2 nN for a cyclooctane fused cyclobutane[16] and ~2 nN for a cyclic acetal fused cyclobutane.[19,32] Thus, the threshold force seemed not to correlate with the identity of the ring sequentially fused to the first cyclobutane ring or the thermodynamic energy of the mechanochemical reaction, but potentially to the stereochemistry of the first cyclobutane.

Mechanoactivation rate constants were calculated based on fits to the individual force curves to account for measurement-to-measurement variation in the contour length of the measured polymers.[33] The derived rate constants were plotted as a function of force (Figure S16). Linear fitting of logarithmic rate constant for the mechanoactivation vs force gave similar slopes of 0.020 ± 0.004, 0.020 ± 0.004, and 0.023 ± 0.004 ln(rate/sec)/pN for **P3**, **P6**, and **P9**, respectively, which experimentally suggests that these mechanochemical ring

Table 1. Polymers of Macrocyclic Mechanophores and Their Force-Response Characterization

Entry	Polymer[a]	Mechanophore units	$M_{n,MALLS}$ (kDa)[b]	Mechanophore mol %[c]	Threshold Force (pN)[d]	Measured Extension %[e]	Calculated Extension %[f]
1	**P1**	**LD**	35	7	1942	1.5 ± 0.2	6.7
2	**P2**	**LD**	27	14	1903	7.2 ± 1.6	12.9
3	**P3**	**LD**	39	63	1910	35.8 ± 2	44.1
4	**P4**	**BLD**	24	9	1687	4.6 ± 0.9	3.6
5	**P5**	**BLD**	20	29	1800	9.0 ± 2.0	10.3
6	**P6**	**BLD**	39	55	1800	16.3 ± 0.9	16.9
7	**P7**	**NLD**	36	18	1893	8.3 ± 0.1	7.9
8	**P8**	**NLD**	58	33	1908	14.7 ± 1.1	13.2
9	**P9**	**NLD**	24	46.5	1920	17.7 ± 0.9	17.2

[a]ROMP was run in reagent grade $CHCl_3$ under nitrogen at 40°C. [b]Determined by GPC MALLS analysis in THF. [c]Determined by H NMR spectroscopy. [d]Determined by SMFS plateau fitting. [e]Determined by SMFS curve fitting. [f]Determined by AISMD modeling. For **LD**, the transition to the all-*E* tetraene was modeled; for **BLD**, the transition to the *Z*, *Z* diene was modeled; for **NLD**, the transition to the *E*, *E* diene was modeled.

https://doi.org/10.1021/jacs.1c05857

opening reactions occur via a similar mechanism. To calculate the rate differences between each mechanophore, these force-rate fits were extrapolated to 1.8 nN for each species (Table S14). At this force, rate constants of 1.0, 4.3, and 1.3 s^{-1} were obtained for **LD**, **BLD**, and **NLD**, respectively.

Crystal structures of the three ladder mechanophores reveal that the first rungs have similar lengths, about 1.57 Å (Figure 2). But the second rungs exhibit larger variation with

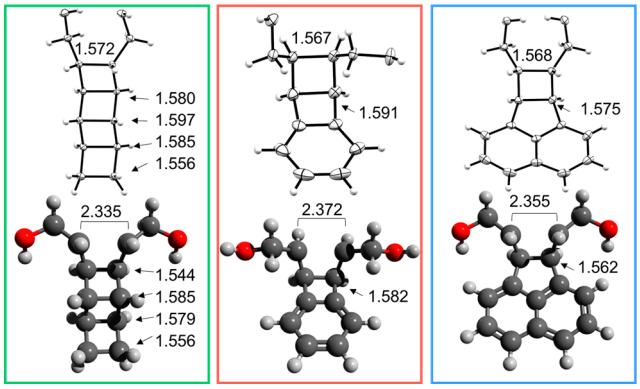

Figure 2. Comparison between the bond lengths for each of the mechanophore diol crystal structures and the transition states, computed at B3LYP+D3/6-31G(d) level. Note that the structures were optimized as the diacetoxy-mechanophore species, but they are rendered here as the corresponding diol for visual clarity of comparison.

increasing lengths of 1.580, 1.591, and 1.575 Å for **LD**, **BLD**, and **NLD** respectively, as affected by the structure of the next fused ring. With these empirical ground state structures in hand, we sought to computationally determine the length change in the first bond in the TS structures using B3LYP +D3/6-31G(d) (Figure 2). The first bond length increases by 0.76, 0.81, and 0.77 Å in the diacetoxy derivatives of **LD**, **BLD**, and **NLD**, respectively. This suggests that the mechanism of activation is very similar for these mechanophores. The activation energy at 2.0 nN for **LD**, **BLD**, and **NLD** was calculated by CASPT2/cc-pVTZ on B3LYP+D3/6-31G(d) geometries to be 17.1, 15.0, and 16.7 kcal/mol. The ~2 kcal/mol higher activation energy of **LD** and **NLD** than **BLD** is consistent with the experimentally observed ~100 pN higher threshold force.

With relatively early TS's, the bond strength of the second rung would have a much weaker effect on the mechanoactivation than the first bond. We calculated the force-modified reaction coordinates for each mechanophore at 2.0 nN (Figure 3). Application of force not only significantly lowers the activation energy for each mechanophore but also shifts the first TS earlier as more force is applied. The distance in mass-weighted coordinates between the reactant and TS is similar for each mechanophore. Taken together, all the experimental and computational data suggest that the cyclobutane-ladder mechanophore activation occurs with an early transition state and the chemical features of the first rung are the primary determinant of ring opening forces in these systems.

In our previous designs of ROMPed mechanophore monomers (Scheme 1), mechanoactivation led to the formation of conjugated polymers, which makes it difficult to analyze the stereochemistry of the mechanically generated dienes. With the mechanophore diols **1**, **3**, and **5** on hand, we

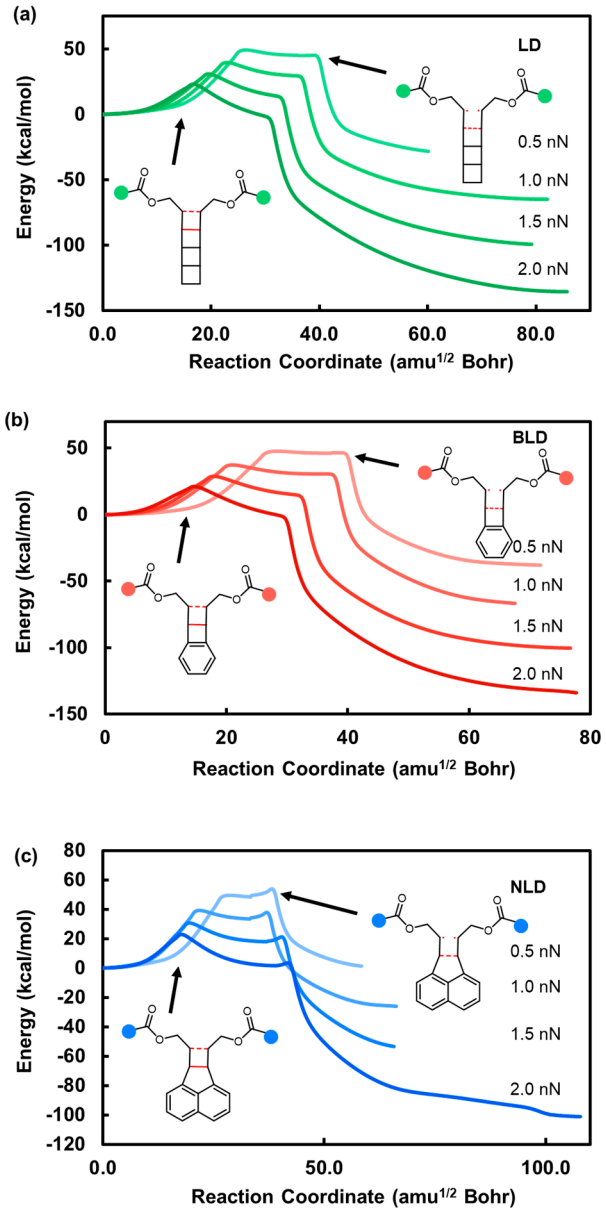

Figure 3. Force-modified reaction coordinates calculated at the B3LYP+D3/6-31(d) level for the full ring opening of the first cyclobutane ring at 0.5, 1.0, 1.5, and 2.0 nN for (a) **LD**, (b) **BLD**, (c) **NLD**.

also synthesized poly(methyl acrylate) with chain-centered mechanophores, which were then sonoactivated. ^{1}H NMR analysis of the mechanochemical products revealed that the generated diene from **BLD** is 80% *Z* and 20% *E*, and that from **NLD** is 100% *E*. Considering the different configuration of **BLD** (*endo*) and **NLD** (*exo*), this result indicates 80% and 100% stereochemical retention for **BLD** and **NLD** mechanoactivation, respectively. From our previous experimental and computational study, we have confirmed that the first pair of generated dienes from **LD** is 100% *E*, completely retaining stereochemistry, and the stereochemical outcome of ladderane mechanochemistry is controlled by a dynamic effect.[10] With the knowledge of the product stereochemistry, we can more accurately computationally calculate the percentage of elongation in polymer contour length upon mechanoactivation. We measured the polymer contour elongation exper-

imentally by fitting a freely joined chain model to the enthalpic distortion region of each force−extension curve before and after the activation plateau. We carried out *ab initio* steered molecular dynamics simulations (AISMD) to calculate the contour lengths of each repeat unit before and after mechanoactivation with an adaptive applied force of 1.9 nN at the B3LYP/6-31G(d) level theory. By using molecular dynamics with explicit forces rather than COGEF to determine repeat unit contour lengths, we obtained a contour length that was averaged over the conformational ensemble accessible at real temperatures and that accounted for the enthalpic distortion resulting from applied force. AISMD contour length prediction of the mechanophore-macrocycle and cyclooctene copolymers **3**, **6**, and **9** showed contour length increase of 44.1, 16.9, and 17.2% respectively (Table 1), which closely matches the experimental results (Table 1). The good agreement supports a match between the activated products from SMFS experiments and those generated during sonication. Calculation indicates that the ROMP polymechanophore homopolymers shown in Scheme 1 have even more dramatic contour length changes with 215%, 89%, and 97% increase for polyladderane, polybenzoladderene, and polynaphthaladderene, respectively (Table S2), even though their direct investigation by SMFS was unsuccessful. Since the "hidden length" released upon mechanophore activation can relieve localized strain,[20,34] these mechanophores may impart intriguing mechanical properties in aptly designed network materials, which we are currently developing.

Retracing experiments of all the polymers showed full hysteresis, suggesting the mechanoactivations were irreversible as expected, but **P9** displayed a more gradual relaxation (slower reduction in stress per reduction in strain) than those of **P6** or **P3** (Figure 4A). COGEF modeling of the contour length relaxation of the ring-opened diacetoxy-**NLD** shows a distinct conformational energy profile resulting from steric clash from the close benzylic protons on the generated diene at the *peri* positions of naphthalene, giving rise to a more gradual reduction in stress at each reduction in strain (Figure 4B). This observation manifests again how molecular properties impact macromolecular behaviors (here, stress relaxation) at a longer length scale, reinforcing the idea that design elements in molecular architecture can be translated to tangible, macroscopic properties.[35]

CONCLUSION

Using SMFS and computation, we have quantitatively studied the mechanochemistry of a series of closely related ladder-type cyclobutane mechanophores to elucidate their reactivity−structure relationships. Their threshold activation force and transition states are insensitive to the nature of the ring fused to cyclobutane but dependent on the steric or electronic properties of the first bond to break in cyclobutane. Multicyclic cyclobutane-based motifs have been increasingly leveraged to induce polymer backbone transformations and as gating elements to enable latent reactivity until an adequate mechanical stimulus is applied.[20,32,36,37] An understanding of the mechanochemistry of the multicyclic fused rings and the mechanical behaviors of their polymers will facilitate the future design of such intriguing mechanophores and the translation of the molecular behaviors to macroscopic properties as force-responsive materials.

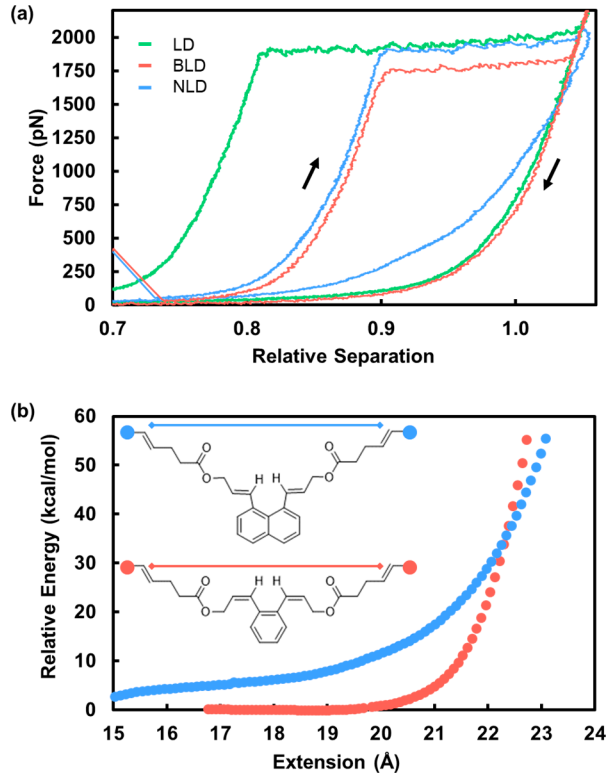

Figure 4. (a) Representative retracing force curves of **P3** (green), **P6** (red), and **P9** (blue) obtained by SMFS at a retraction velocity of 300 nm/s. (b) COGEF modeling comparing the relaxation of the ring-opened **BLD** (red) and **NLD** (blue), calculated at the PM6 level.

ASSOCIATED CONTENT

Supporting Information

The Supporting Information is available free of charge at https://pubs.acs.org/doi/10.1021/jacs.1c05857.

Detailed descriptions of synthetic procedures, ^{1}H and ^{13}C NMR spectra of new compounds and polymers, GPC analysis, SMFS, computational details, and crystallographic data for **1**, **3**, and **5** (PDF)

Accession Codes

CCDC 1953038, 1993456, and 1993502 contain the supplementary crystallographic data for this paper. These data can be obtained free of charge via www.ccdc.cam.ac.uk/data_request/cif, or by emailing data_request@ccdc.cam.ac.uk, or by contacting The Cambridge Crystallographic Data Centre, 12 Union Road, Cambridge CB2 1EZ, UK; fax: +44 1223 336033.

AUTHOR INFORMATION

Corresponding Authors

Todd J. Martínez − *Department of Chemistry, Stanford University, Stanford, California 94305, United States; SLAC National Accelerator Laboratory, Menlo Park, California 94025, United States;* orcid.org/0000-0002-4798-8947; Email: toddmtz@stanford.edu

Stephen L. Craig − *Department of Chemistry, Duke University, Durham, North Carolina 27708, United States;* orcid.org/0000-0002-8810-0369; Email: stephen.craig@duke.edu

Yan Xia − *Department of Chemistry, Stanford University, Stanford, California 94305, United States;* orcid.org/0000-0002-5298-748X; Email: yanx@stanford.edu

Authors

Matías Horst − *Department of Chemistry, Stanford University, Stanford, California 94305, United States;* orcid.org/0000-0002-9794-5355

Jinghui Yang − *Department of Chemistry, Stanford University, Stanford, California 94305, United States;* orcid.org/0000-0002-6957-6265

Jan Meisner − *Department of Chemistry, Stanford University, Stanford, California 94305, United States;* orcid.org/0000-0002-1301-2612

Tatiana B. Kouznetsova − *Department of Chemistry, Duke University, Durham, North Carolina 27708, United States*

Complete contact information is available at: https://pubs.acs.org/10.1021/jacs.1c05857

Notes

The authors declare no competing financial interest.

■ ACKNOWLEDGMENTS

This work was supported by the U.S. Army Research Office under grant number W911NF-15-1-0525 (Y.X. and T.M.) and the National Science Foundation under the grant number CHE-1808518 (S.L.C.). M. H. is supported by a National Defense Science and Engineering Graduate Fellowship. J. Y. is supported by a Stanford Graduate Fellowship. JM thanks the Deutsche Forschungsgemeinschaft (project number 419817859) for financial support. Single-crystal X-ray diffraction experiments were performed at beamline 12.2.1 at the Advanced Light Source (ALS). The ALS is supported by the Director, Office of Science, Office of Basic Energy Science, of the U.S. Department of Energy under contract no. DE-AC02-05CH11231. This work used the XStream computational resource, supported by the National Science Foundation Major Research Instrumentation program (ACI-1429830). Some of the computation was performed on the Sherlock cluster. We would like to thank Stanford University and the Stanford Research Computing Center for providing computational resources and support that contributed to these research results. We thank Umicore for a gift of Grubbs catalyst.

■ REFERENCES

(1) Hickenboth, C. R.; Moore, J. S.; White, S. R.; Sottos, N. R.; Baudry, J.; Wilson, S. R. Biasing Reaction Pathways with Mechanical Force. *Nature* **2007**, *446*, 423−427.

(2) Wang, J.; Kouznetsova, T. B.; Craig, S. L. Reactivity and Mechanism of a Mechanically Activated *Anti* -Woodward−Hoffmann−DePuy Reaction. *J. Am. Chem. Soc.* **2015**, *137*, 11554−11557.

(3) Wang, J.; Kouznetsova, T. B.; Niu, Z.; Ong, M. T.; Klukovich, H. M.; Rheingold, A. L.; Martinez, T. J.; Craig, S. L. Inducing and Quantifying Forbidden Reactivity with Single-Molecule Polymer Mechanochemistry. *Nat. Chem.* **2015**, *7*, 323−327.

(4) Akbulatov, S.; Tian, Y.; Huang, Z.; Kucharski, T. J.; Yang, Q.-Z.; Boulatov, R. Experimentally Realized Mechanochemistry Distinct from Force-Accelerated Scission of Loaded Bonds. *Science* **2017**, *357*, 299−303.

(5) Stevenson, R.; De Bo, G. Controlling Reactivity by Geometry in Retro-Diels−Alder Reactions under Tension. *J. Am. Chem. Soc.* **2017**, *139*, 16768−16771.

(6) McFadden, M. E.; Robb, M. J. Force-Dependent Multicolor Mechanochromism from a Single Mechanophore. *J. Am. Chem. Soc.* **2019**, *141*, 11388−11392.

(7) Klukovich, H. M.; Kouznetsova, T. B.; Kean, Z. S.; Lenhardt, J. M.; Craig, S. L. A Backbone Lever-Arm Effect Enhances Polymer Mechanochemistry. *Nat. Chem.* **2013**, *5*, 110−114.

(8) Wang, J.; Kouznetsova, T. B.; Kean, Z. S.; Fan, L.; Mar, B. D.; Martínez, T. J.; Craig, S. L. A Remote Stereochemical Lever Arm Effect in Polymer Mechanochemistry. *J. Am. Chem. Soc.* **2014**, *136*, 15162−15165.

(9) Wollenhaupt, M.; Schran, C.; Krupička, M.; Marx, D. Force-Induced Catastrophes on Energy Landscapes: Mechanochemical Manipulation of Downhill and Uphill Bifurcations Explains the Ring-Opening Selectivity of Cyclopropanes. *ChemPhysChem* **2018**, *19*, 837−847.

(10) Chen, Z.; Zhu, X.; Yang, J.; Mercer, J. A. M.; Burns, N. Z.; Martinez, T. J.; Xia, Y. The Cascade Unzipping of Ladderane Reveals Dynamic Effects in Mechanochemistry. *Nat. Chem.* **2020**, *12*, 302−309.

(11) Beyer, M. K. The Mechanical Strength of a Covalent Bond Calculated by Density Functional Theory. *J. Chem. Phys.* **2000**, *112*, 7307−7312.

(12) Klein, I. M.; Husic, C. C.; Kovács, D. P.; Choquette, N. J.; Robb, M. J. Validation of the CoGEF Method as a Predictive Tool for Polymer Mechanochemistry. *J. Am. Chem. Soc.* **2020**, *142*, 16364−16381.

(13) Sotomayor, M.; Schulten, K. Single-Molecule Experiments in Vitro and in Silico. *Science* **2007**, *316*, 1144−1148.

(14) Ribas-Arino, J.; Shiga, M.; Marx, D. Understanding Covalent Mechanochemistry. *Angew. Chem., Int. Ed.* **2009**, *48*, 4190−4193.

(15) Ong, M. T.; Leiding, J.; Tao, H.; Virshup, A. M.; Martínez, T. J. First Principles Dynamics and Minimum Energy Pathways for Mechanochemical Ring Opening of Cyclobutene. *J. Am. Chem. Soc.* **2009**, *131*, 6377−6379.

(16) Stauch, T.; Dreuw, A. Quantum Chemical Strain Analysis For Mechanochemical Processes. *Acc. Chem. Res.* **2017**, *50*, 1041−1048.

(17) Wang, J.; Kouznetsova, T. B.; Niu, Z.; Rheingold, A. L.; Craig, S. L. Accelerating a Mechanically Driven *Anti* -Woodward−Hoffmann Ring Opening with a Polymer Lever Arm Effect. *J. Org. Chem.* **2015**, *80*, 11895−11898.

(18) Kryger, M. J.; Munaretto, A. M.; Moore, J. S. Structure−Mechanochemical Activity Relationships for Cyclobutane Mechanophores. *J. Am. Chem. Soc.* **2011**, *133*, 18992−18998.

(19) Wang, J.; Kouznetsova, T. B.; Boulatov, R.; Craig, S. L. Mechanical Gating of a Mechanochemical Reaction Cascade. *Nat. Commun.* **2016**, *7*, 13433.

(20) Tian, Y.; Cao, X.; Li, X.; Zhang, H.; Sun, C.-L.; Xu, Y.; Weng, W.; Zhang, W.; Boulatov, R. A Polymer with Mechanochemically Active Hidden Length. *J. Am. Chem. Soc.* **2020**, *142*, 18687−18697.

(21) Chen, Z.; Mercer, J. A. M.; Zhu, X.; Romaniuk, J. A. H.; Pfattner, R.; Cegelski, L.; Martinez, T. J.; Burns, N. Z.; Xia, Y. Mechanochemical Unzipping of Insulating Polyladderene to Semiconducting Polyacetylene. *Science* **2017**, *357*, 475−479.

(22) Su, J. K.; Feist, J. D.; Yang, J.; Mercer, J. A. M.; Romaniuk, J. A. H.; Chen, Z.; Cegelski, L.; Burns, N. Z.; Xia, Y. Synthesis and Mechanochemical Activation of Ladderene−Norbornene Block Copolymers. *J. Am. Chem. Soc.* **2018**, *140*, 12388−12391.

(23) Yang, J.; Horst, M.; Romaniuk, J. A. H.; Jin, Z.; Cegelski, L.; Xia, Y. Benzoladderene Mechanophores: Synthesis, Polymerization, and Mechanochemical Transformation. *J. Am. Chem. Soc.* **2019**, *141*, 6479−6483.

(24) Yang, J.; Horst, M.; Werby, S. H.; Cegelski, L.; Burns, N. Z.; Xia, Y. Bicyclohexene- *Peri* -Naphthalenes: Scalable Synthesis, Diverse Functionalization, Efficient Polymerization, and Facile Mechanoactivation of Their Polymers. *J. Am. Chem. Soc.* **2020**, *142*, 14619−14626.

(25) Suslick, K. S. Sonochemistry. *Science* **1990**, *247*, 1439−1445.

(26) Caruso, M. M.; Davis, D. A.; Shen, Q.; Odom, S. A.; Sottos, N. R.; White, S. R.; Moore, J. S. Mechanically-Induced Chemical Changes in Polymeric Materials. *Chem. Rev.* **2009**, *109*, 5755−5798.

(27) Gossweiler, G. R.; Kouznetsova, T. B.; Craig, S. L. Force-Rate Characterization of Two Spiropyran-Based Molecular Force Probes. *J. Am. Chem. Soc.* **2015**, *137*, 6148−6151.
(28) Barbee, M. H.; Kouznetsova, T.; Barrett, S. L.; Gossweiler, G. R.; Lin, Y.; Rastogi, S. K.; Brittain, W. J.; Craig, S. L. Substituent Effects and Mechanism in a Mechanochemical Reaction. *J. Am. Chem. Soc.* **2018**, *140*, 12746−12750.
(29) Sha, Y.; Zhang, Y.; Xu, E.; Wang, Z.; Zhu, T.; Craig, S. L.; Tang, C. Quantitative and Mechanistic Mechanochemistry in Ferrocene Dissociation. *ACS Macro Lett.* **2018**, *7*, 1174−1179.
(30) Razgoniaev, A. O.; Glasstetter, L. M.; Kouznetsova, T. B.; Hall, K. C.; Horst, M.; Craig, S. L.; Franz, K. J. Single-Molecule Activation and Quantification of Mechanically Triggered Palladium−Carbene Bond Dissociation. *J. Am. Chem. Soc.* **2021**, *143*, 1784−1789.
(31) Zhang, Y.; Wang, Z.; Kouznetsova, T. B.; Sha, Y.; Xu, E.; Shannahan, L.; Fermen-Coker, M.; Lin, Y.; Tang, C.; Craig, S. L. Distal Conformational Locks on Ferrocene Mechanophores Guide Reaction Pathways for Increased Mechanochemical Reactivity. *Nat. Chem.* **2021**, *13*, 56−62.
(32) Lin, Y.; Kouznetsova, T. B.; Craig, S. L. Mechanically Gated Degradable Polymers. *J. Am. Chem. Soc.* **2020**, *142*, 2105−2109.
(33) Kouznetsova, T. B.; Wang, J.; Craig, S. L. Combined Constant-Force and Constant-Velocity Single-Molecule Force Spectroscopy of the Conrotatory Ring Opening Reaction of Benzocyclobutene. *ChemPhysChem* **2017**, *18*, 1486−1489.
(34) Bowser, B. H.; Wang, S.; Kouznetsova, T. B.; Beech, H. K.; Olsen, B. D.; Rubinstein, M.; Craig, S. L. Single-Event Spectroscopy and Unravelling Kinetics of Covalent Domains Based on Cyclobutane Mechanophores. *J. Am. Chem. Soc.* **2021**, *143*, 5269−5276.
(35) Wang, S.; Beech, H. K.; Bowser, B. H.; Kouznetsova, T. B.; Olsen, B. D.; Rubinstein, M.; Craig, S. L. Mechanism Dictates Mechanics: A Molecular Substituent Effect in the Macroscopic Fracture of a Covalent Polymer Network. *J. Am. Chem. Soc.* **2021**, *143*, 3714−3718.
(36) Hsu, T.-G.; Zhou, J.; Su, H.-W.; Schrage, B. R.; Ziegler, C. J.; Wang, J. A Polymer with "Locked" Degradability: Superior Backbone Stability and Accessible Degradability Enabled by Mechanophore Installation. *J. Am. Chem. Soc.* **2020**, *142*, 2100−2104.
(37) Yang, J.; Xia, Y. Mechanochemical Generation of Acid-Degradable Poly(Enol Ether)s. *Chem. Sci.* **2021**, *12*, 4389−4394.

https://doi.org/10.1021/jacs.1c05857